Cellular/Molecular

Activity-Dependent Internalization of Glun2B-Containing NMDARs Is Required for Synaptic Incorporation of Glun2A and Synaptic Plasticity

Granville P. Storey, Raul Riquelme, and Andres Barria
Department of Neurobiology and Biophysics, University of Washington School of Medicine, Seattle, Washington 98195-7290

NMDA-type glutamate receptors are heterotetrameric complexes composed of two GluN1 and two GluN2 subunits. The precise composition of the GluN2 subunits determines the channel's biophysical properties and influences its interaction with postsynaptic scaffolding proteins and signaling molecules involved in synaptic physiology and plasticity. The precise regulation of NMDAR subunit composition at synapses is crucial for proper synaptogenesis, neuronal circuit development, and synaptic plasticity, a cellular model of memory formation. In the forebrain during early development, NMDARs contain solely the GluN2B subunit, which is necessary for proper synaptogenesis and synaptic plasticity. In rodents, GluN2A subunit expression begins in the second postnatal week, replacing GluN2B-containing NMDARs at synapses in an activity- or sensory experience-dependent process. This switch in NMDAR subunit composition at synapses alters channel properties and reduces synaptic plasticity. The molecular mechanism regulating the switch remains unclear. We have investigated the role of activity-dependent internalization of GluN2B-containing receptors in shaping synaptic NMDAR subunit composition. Using molecular, pharmacological, and electrophysiological approaches in cultured organotypic hippocampal slices from rats of both sexes, we show that the process of incorporating GluN2A-containing NMDAR receptors requires activity-dependent internalization of GluN2B-containing NMDARs. Interestingly, blockade of GluN2A synaptic incorporation was associated with impaired potentiation of AMPA-mediated synaptic transmission, suggesting a potential coupling between the trafficking of AMPARs into synapses and that of GluN2A-containing NMDARs. These insights contribute to our understanding of the molecular mechanisms underlying synaptic trafficking of glutamate receptors and synaptic plasticity. They may also have implications for therapeutic strategies targeting NMDAR function in neurological disorders.

Key words: **glutamate receptors; NMDA receptor; synaptic plasticity; trafficking of glutamate receptors**

Significance Statement

NMDARs play a critical role in synaptogenesis, synaptic stability, and activity-dependent regulation of synaptic strength. The developmental switch in their GluN2 subunits composition is part of normal synapse development and crucial for proper synaptic physiology, plasticity, and the formation of functional neuronal circuits, though the mechanisms governing it remain unclear. We show that internalization of GluN2B-containing NMDARs is required for synaptic incorporation of GluN2A-containing receptors. This process can be induced by long-term potentiation and requires Ca^{+2}. Notably, GluN2A trafficking to synapses is linked to the incorporation of AMPA-type glutamate receptors, suggesting a shared pathway for synaptic incorporation. These findings provide greater insight into the molecular mechanisms behind glutamate receptor trafficking and synaptic plasticity, potentially informing therapeutic strategies for neurological disorders.

Introduction

In many brain regions, synapses undergo a developmental switch in the subunit composition of NMDA receptors (Carmignoto and Vicini, 1992; Stocca and Vicini, 1998; Philpot et al., 2001; Yashiro and Philpot, 2008). During early development, NMDA receptors are composed of two of the obligatory GluN1 subunits, which is present in all NMDARs, and two GluN2B subunits, forming a tetramer (Hansen et al., 2021). GluN2B plays a crucial role in neural development, synaptic plasticity, and overall animal viability (Kutsuwada et al., 1996; Barria and Malinow, 2005;

Received May 2, 2024; revised Nov. 6, 2024; accepted Nov. 9, 2024.
Author contributions: G.P.S. and A.B. designed research; G.P.S. and R.R. performed research; G.P.S., R.R., and A.B. analyzed data; A.B. wrote the paper.
This work was supported by the National Science Foundation (NSF) grant NSF-IOS-2224262 (A.B.).
The authors declare no competing financial interests.
Correspondence should be addressed to Andres Barria at barria@uw.edu.
https://doi.org/10.1523/JNEUROSCI.0823-24.2024

Ewald et al., 2008). It mediates prolonged channel openings, leading to long-lasting currents and subsequent prolonged postsynaptic depolarization. Additionally, its large intracellular carboxy-terminal domain allows the anchoring of active calcium/calmodulin-dependent kinase II (CaMKII; Strack et al., 2000; Mayadevi et al., 2002), a necessary step for long-term potentiation (LTP) of synaptic transmission mediated by AMPAR-type glutamate receptors (AMPARs; Barria and Malinow, 2005; Zhou et al., 2007; Halt et al., 2012). Post-Golgi trafficking of GluN2B-containing NMDARs is regulated by palmitoylation (Hayashi et al., 2009; Mattison et al., 2012), while Wnt signaling can control the movement of GluN2B-containing NMDA receptors toward the neuronal surface (Cerpa et al., 2011; McQuate et al., 2017). From there, they can be incorporated into synapses by diffusion, independently of synaptic activity (Barria and Malinow, 2002; McQuate and Barria, 2020). GluN2B can be internalized in an activity-dependent manner through a YEKL motif in its intracellular carboxy-terminal domain, which interacts with the AP-2 complex (Lavezzari et al., 2003, 2004).

The expression of other GluN2 subunits is developmentally regulated and region specific (Akazawa et al., 1994; Monyer et al., 1994). In the hippocampus, cortex, and other forebrain regions of rodents, GluN2A expression increases after the second postnatal week, leading to a partial replacement of GluN2B-containing NMDARs with those containing GluN2A at synapses (Carmignoto and Vicini, 1992; Stocca and Vicini, 1998; Yashiro and Philpot, 2008; Storey et al., 2011). Consequently, mature synaptic NMDARs exhibit a range of compositions, including diheteromeric GluN1/GluN2B, diheteromeric GluN1/GluN2A, as well as triheteromeric GluN1/GluN2B/GluN2A receptors, with their ratios varying across different synapses, brain regions, and developmental stages (Hansen et al., 2021).

Quantitative assessments of the relative abundance of different NMDAR populations in the intact juvenile hippocampus has been difficult. Biochemical studies in hippocampal tissue estimate that ~60–85% of GluN2A and GluN2B subunits form diheteromeric receptors (GluN1/GluN2A or GluN1/GluN2B), while the remaining 15–40% contribute to triheteromeric receptor populations (Al-Hallaq et al., 2007). However, electrophysiological approaches in cultured dissociated neurons report a higher proportion of triheteromeric receptors, ~66% (Tovar et al., 2013).

The switch in subunit composition of synaptic NMDARs alters the NMDAR-mediated current, as receptors containing GluN2A desensitize faster and exhibit faster opening and closing kinetics compared with those containing solely GluN2B (Dingledine et al., 1999). It also reduces synaptic plasticity, as the carboxy-terminal domain of GluN2A lacks a binding sequence for CaMKII (Omkumar et al., 1996; Mayadevi et al., 2002; Barria and Malinow, 2005). Different rules seem to govern trafficking of GluN2A-containing receptors into synapses, as they require synaptic activity acting on pre-existing GluN2B-containing NMDARs for synaptic incorporation (Barria and Malinow, 2002). This process aligns with the observation that GluN2A-containing receptors are predominantly localized to synaptic sites (Groc et al., 2006; Kellermayer et al., 2018). Sensory experience is also required for the proper switch in the GluN2 subunit composition of synaptic NMDARs, with dark-reared animals maintaining a high GluN2B/GluN2A ratio at synapses in the visual cortex (Quinlan et al., 1999a,b; Philpot et al., 2001). The carboxy-terminal domain of GluN2A lacks the YEKL motif, which mediates receptor endocytosis in GluN2B, thereby contributing to the greater stability of GluN2A-containing receptors at synapses (Lavezzari et al., 2003, 2004; Sanz-Clemente et al., 2010).

Synaptic incorporation of GluN2A-containing NMDA receptors is typically detected by a decrease in the decay time of evoked excitatory postsynaptic currents (EPSCs). This reduction is commonly observed during the second postnatal week in the hippocampus of rodents—a period characterized by robust synaptogenesis and plasticity (Carmignoto and Vicini, 1992; Stocca and Vicini, 1998; Philpot et al., 2001; Gambrill and Barria, 2011; Storey et al., 2011). Dysregulation of the switch between GluN2B and GluN2A subunits could significantly impact synaptic plasticity and the development of neuronal properties (Gambrill and Barria, 2011), ultimately affecting the formation of functional brain circuits. In a mouse model of fragile X syndrome, knock-out of the FMR1 gene results in early expression and synaptic incorporation of GluN2A subunits (Banke et al., 2024). This alters the synaptic physiology and plasticity of neurons occurring during a critical period when synapses and circuits are developing, suggesting that dysregulation of the GluN2B/GluN2A switch may contribute to the formation of pathological circuits in the fFragile X mouse model.

The process through which the synaptic switch in GluN2 subunits is coordinated remains largely unknown. In this study, we specifically investigated whether the synaptic activity-induced removal of GluN2B is a prerequisite for the incorporation of GluN2A-containing receptors into synapses and examined the specific requirements for GluN2A synaptic incorporation.

Materials and Methods

Dissociated neurons and slice cultures and transfections. Organotypic hippocampal slices were prepared from p6 Sprague Dawley rats of both sexes as described previously (Opitz-Araya and Barria, 2011) and cultured at 35°C and 5% CO_2 in medium containing 8.4 g/L MEM, 20% Horse serum heat inactivated, 1 mM L-glutamine, 1 mM $CaCl_2$, 2 mM $MgSO_4$, 1 mg/L insulin, 0.00125% ascorbic acid, 13 mM D-glucose, 5.2 mM $NaHCO_3$, and 30 mM and Hepes.

After 3–5 d in culture, slices were transfected using a biolistic particle delivery system (Woods and Zito, 2008) and cultured for an additional 48–72 h to allow expression of recombinant proteins. For experiments requiring treatment of the slices with APV (Tocris), the drug was added immediately after transfection and replenished every 24 h. In experiments requiring treatment with the antennapedia fusion peptides, 5 μM of the peptide was added to the slice culture media 2 h before recording. In experiments requiring treatment with the casein kinase II inhibitor, TBB (Tocris), 10 μM was added to the slice culture media 2 h before recording. In the case of TBB, 10 μM was also added to the bath solution during recording.

Dissociated hippocampal neuron cultures were prepared from hippocampi collected from mice CB57BL/6G of both sexes at postnatal day 1 (P1). Tissue from 3–4 animals was collected in cold dissection medium containing Hanks' Plus HBBSS+, 10 mM HEPES, 33.3 mM glucose, 0.3% BSA, and 12 mM MgSO4, processed, and neurons plated at a density of 200,000 cells per 35 mm plates. Neurons were cultured in neuronal medium containing MEM, 25 mM HEPES, 20 mM glucose, 10% Horse serum, 2% B27, 1% sodium pyruvate, GlutaMAX, and 1% penicillin/streptomycin. After 6 d in vitro (DIV), neurons were supplemented with 20 μM fluorodeoxyuridine. Neurons were used between 12 and 18 DIV. Dissociated neurons were transfected using Lipofectamine 2000 (Invitrogen) and constructs expressed for 24–36 h.

Electrophysiology. Whole-cell recordings were obtained from transfected or nontransfected neurons under visual guidance using epifluorescence and transmitted light illumination from an Olympus BX51W1 microscope. The recording chamber was perfused with artificial cerebrospinal fluid containing the following: 119 mM NaCl, 2.5 mM KCl, 4 mM $CaCl_2$, 4 mM $MgCl_2$, 26 mM $NaHCO_3$, 1 mM NaH_2PO_4, 11 mM glucose, 100 μM picrotoxin (Tocris), 2 μM 2-chloroadenosine, pH 7.4, and gassed with 5% CO_2/95% O_2. Recordings were performed at room

temperature (20–25°C), except in rapid incorporation experiments which were performed at 27°C. Whole-cell recording pipettes (3–6 MΩ) were filled with intracellular recording solution containing the following (in mM): 115 cesium methanesulfonate, 20 CsCl, 10 HEPES, 2.5 $MgCl_2$, 2 MgATP, 2 Na_2ATP, 0.4 Na_3GTP, 10 sodium phosphocreatine, 5 QX-314, and 0.6 EGTA, pH 7.25, and 310 mmol/kg. Whole-cell recordings were made using a MultiClamp 700B computer-controlled amplifier (Axon Instruments). Synaptic responses were evoked by bipolar cluster electrodes (FHC) placed over Schaffer collateral fibers ~200–300 µm from targeted CA1 neuron. NMDAR kinetics was measured as time to half-decay (100% peak current to 50% remaining current) obtained from 20–50 evoked EPSCs while holding the cell +40 mV in the presence of 2 µM NBQX. In experiments measuring incorporation index of recombinant GluN2A, the NMDAR amplitude was measured as the mean current from a 50 ms window 110 ms after the stimulus artifact in evoked EPSCs recorded while holding the cell at −60 mV. The peak amplitude of the EPSC is mediated by endogenous AMPARs and was used to normalize the recombinant NMDAR response.

Fluorescence imaging. Detection of SEP-tagged GluN2B subunits of the NMDAR was done in cultured dissociated neurons obtained from three to four P1 animals and cotransfected with GluN2B-SEP, GluN1, and YEKL or control peptides. Fluorescence *Z*-stacks were taken every 30 s in a Zeiss710 confocal microscope. One cell per dish was imaged and experiments were repeated in neurons coming from at least three different preparations. Fluorescence images were analyzed using ImageJ, and fluorescence values normalized to the average of baseline images.

Plasmids and peptide construction. A mammalian expression plasmid carrying the YEKL domain of GluN2B was constructed by fusing mCherry to the GluN2B carboxy-terminal at A1315 and incorporating a stop codon after L1475, thus eliminating the PDZ binding motif. A control plasmid was created by inserting a stop codon after V1471, thus also eliminating the YEKL motif.

GluN2A and GluN1 N598R were tagged with GFP and expressed using a mammalian expression plasmid as reported previously (Barria and Malinow, 2002).

Antennapedia peptides were synthesized by Genemed Synthesis containing the following amino acid sequences: RQIKIWFQNRRMK WKKNGHVYEKLSSIE for the Ant-YEKL peptide and RQIKIWFQ NRRMKWKKNGHVAEKLSSIE for the control Ant-AEKL peptide.

Experimental design and statistical analysis. Whole-cell recordings were obtained from one or two neurons per hippocampal slice. Batches of organotypic cultured slices were obtained from three to six Sprague Dawley rats of both sexes at P6 and cultured for 6–8 d. All results are presented as mean ± SEM.

Statistical comparisons between paired recordings (Figs. 1, 2) were conducted using a nonparametric Wilcoxon test, while comparisons between control and treated conditions (Figs. 5, 6) used an unpaired nonparametric Mann–Whitney test. A two-tailed p value was applied, with the specific p values indicated in each figure legend. Statistical significance was defined as $p < 0.05$.

For comparisons involving multiple treatments (Figs. 2–4), a one-way ANOVA was performed, followed by Tukey's post hoc test. The F and p values for each ANOVA are listed in the figure legends, along with the specific p values from Tukey's post hoc test. All data were analyzed using Prism software.

Results

Blockade of activity-dependent internalization of endogenous GluN2B-containing receptors

Activity-dependent internalization of GluN2B-containing NMDARs requires the interaction of the endocytic motif YEKL present only in the C terminus of the GluN2B subunit and the clathrin adaptor protein AP-2. Phosphorylation of tyrosine 1472 within the endocytic motif by Src kinases prevents this interaction, thereby stabilizing the surface expression of NMDARs (Roche et al., 2001; Lavezzari et al., 2003; Zhang et al., 2008; Sanz-Clemente et al., 2010).

We aimed to disrupt the internalization of GluN2B-containing NMDARs in CA1 pyramidal neurons by expressing a competing peptide containing the YEKL motif. We hypothesized that this peptide would competitively inhibit the interaction between GluN2B and the AP-2 endocytic machinery, thereby blocking activity-dependent GluN2B internalization and enhancing its presence at synapses.

We specifically targeted the interaction of GluN2B with the endocytic machinery responsible for its activity-dependent internalization, rather than more downstream and general processes, to avoid the broader and potentially less specific impacts associated with altering general endo- and exocytosis mechanisms. We assessed the effectiveness of a peptide containing the YEKL motif in blocking activity-dependent internalization of GluN2B using both electrophysiological and fluorescence imaging assays.

First, we aimed to block the activity-dependent internalization that typically occurs in neurons during culture. We hypothesized that preventing GluN2B internalization would lead to its accumulation at synapses, which could be detected electrophysiologically when compared with nontransfected neurons. Organotypic cultured hippocampal slices (Opitz-Araya and Barria, 2011) were transfected using biolistic (Woods and Zito, 2008) with an mCherry-tagged peptide named YEKL peptide. This peptide contained the last portion of the GluN2B C-tail (amino acids 1,315–1,475) but lacked the PDZ binding domain to prevent interactions with proteins from the MAGUK family (Prybylowski et al., 2005). As a control, a similar construct lacking the YEKL motif (amino acids 1,315–1,471) was utilized. Following 36–60 h of expression, we assessed the impact of these constructs on endogenous synaptic NMDARs by comparing the amplitude of isolated NMDAR-evoked postsynaptic currents (EPSCs) recorded from a transfected neuron and an adjacent nontransfected neuron (paired recordings). EPSCs were evoked by stimulating Schaffer collaterals with bipolar electrodes.

Cells expressing the YEKL peptide exhibited larger (Fig. 1*A*,*B*) and slower (Fig. 1*C*) NMDAR EPSCs compared with adjacent nontransfected cells stimulated under the same conditions. At this developmental stage, the kinetics of decay of NMDAR-mediated EPSCs and their sensitivity to GluN2B-specific allosteric modulators indicate a predominance of GluN2B-containing receptors (Sanchez et al., 2010; Gambrill et al., 2011; Gambrill and Barria, 2011; Gray et al., 2011; Storey et al., 2011; Sanchez et al., 2012; Banke et al., 2024). The increase in the weighted tau is small but significant, as expected for an EPSC already dominated by GluN2B; however, it is consistent with an increased GluN2B to GluN2A ratio at synapses. Neurons transfected with the control peptide showed no increase in amplitude or change in kinetics of the NMDAR-mediated EPSCs compared with adjacent nontransfected cells (Fig. 1*D*–*F*).

We also evaluated whether the YEKL peptide could prevent the internalization of GluN2B-containing NMDARs optically tagged with superecliptic pHluorin (SEP), a pH-sensitive form of GFP. Tagging the GluN2B subunit with SEP allowed us to monitor the surface expression of GluN2B-containing NMDARs and assess the effect of expressing either the YEKL peptide or the control peptide.

Dissociated cultured neurons were cotransfected with GluN1 and GluN2B-SEP along with either the YEKL peptide or control peptide. Imaging was performed in the presence of 1 µM TTX and 2 µM NBQX to block endogenous activity. After establishing a baseline, 0.1 mM glutamate was added to the bath to induce

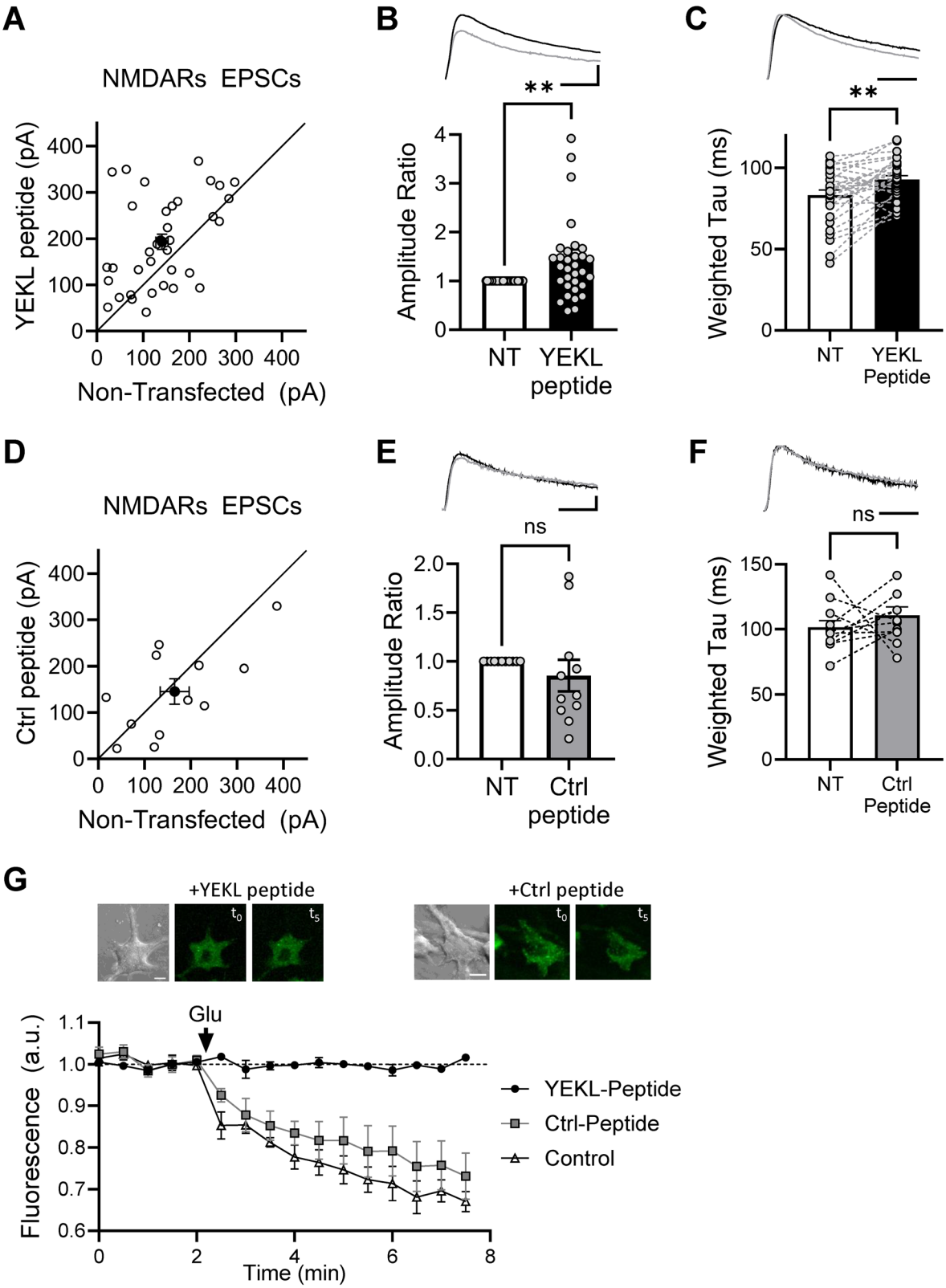

Figure 1. Blockade of endogenous GluN2B-containing receptors internalization by YEKL peptide. ***A***, Paired recordings of neurons transfected with YEKL peptide and control nontransfected (NT) neurons. Peak amplitude of isolated NMDAR-mediated currents recorded at +40 mV and in the presence of 2 µM NBQX from CA1 transfected and control neurons recorded as pairs ($n = 36$ pairs). Optically tagged YEKL peptide was transfected using biolistic and expressed for 2–3 d. Black dot is average ± SEM. ***B***, Top, Sample EPSC traces from a control neuron (gray trace) and a neuron expressing YEKL peptide (black trace) recorded at +40 mV. Calibration: 50 ms and 100 pA. Bottom, Peak amplitude of NMDAR-mediated EPSCs from paired recordings normalized to the amplitude of the control nontransfected (NT) neuron. Statistical significance was determined using Wilcoxon matched pairs test ($p = 0.0049$). ***C***, Top, Sample EPSC traces normalized to peak amplitude from a control neuron (gray trace) and a neuron expressing YEKL peptide (black trace) recorded at +40 mV. Calibration: 50 ms. Bottom, Weighted tau of NMDAR EPSCs from control nontransfected (NT) neurons and neurons expressing YEKL peptide. Statistical significance was determined using Wilcoxon matched pairs test ($p = 0.0012$). ***D***, Paired recordings of neurons transfected with control peptide lacking the YEKL motif and control nontransfected (NT) neurons. Peak amplitude of isolated NMDAR-mediated currents recorded at +40 mV and in

internalization of GluN2B-containing receptors. In neurons coexpressing GluN2B-SEP and the control peptide, or neurons expressing only GluN2B-SEP, the addition of glutamate immediately caused a decrease in surface fluorescence. In contrast, in neurons coexpressing the YEKL peptide, glutamate addition did not trigger internalization of GluN2B-SEP (Fig. 1*G*).

We also investigated the impact of expressing the YEKL peptide on synaptic AMPARs. Surprisingly, blocking the internalization of GluN2B-containing NMDARs led to a decrease in the amplitude of AMPAR-mediated EPSCs compared with adjacent nontransfected neurons (Fig. 2*A*,*C*). This observation could be attributed to the disruption of normal synaptic plasticity. Specifically, it appears that the forward trafficking and synaptic incorporation of AMPARs, which are part of the synaptic maturation process during the culturing period and the expression of the peptides, may be impaired. The expression of the control peptide had no effect on AMPAR-mediated synaptic transmission (Fig. 2*B*,*C*).

To determine if the YEKL peptide affects the removal or recycling of other synaptically relevant receptors, we examined the amplitude of isolated GABA receptor IPSCs. We focused on GABA receptor transmission because GABAR endocytosis is known to be regulated by AP-2 (Kittler et al., 2000; Kneussel, 2002). We hypothesized that if the YEKL peptide lacked specificity for GluN2B, it could interfere with GABAR internalization, potentially leading to their synaptic accumulation.

Recording from pairs consisting of a YEKL-transfected neuron and a nontransfected neighbor, we evoked IPSCs in the presence of 100 µM APV and 2 µM NBQX and compared amplitudes. However, we did not observe any differences in the amplitude of the GABAR IPSCs, leading us to conclude that the removal or recycling of GABA-Rs was not affected by YEKL peptide expression (Figs. 2*D*,*E*).

Altogether, these data suggest that the YEKL peptide competes with the tail of endogenous GluN2B for binding to AP-2, thereby preventing the internalization of synaptic GluN2B receptors. This leads to an increase in the number of synaptic GluN2B-containing NMDARs relative to nontransfected paired cells, consistent with previous reports on the role of the YEKL motif (Lavezzari et al., 2003, 2004). These findings validate the use of the YEKL peptide to interfere with NMDAR internalization. Furthermore, these experiments suggest that the internalization of GluN2B-containing receptors may be coupled to the normal synaptic incorporation of AMPA-type glutamate receptors during the expression period in the cultured slice.

YEKL peptide blocks synaptic incorporation of recombinant GluN2A-containing receptors

In rodents, expression of the GluN2A subunits starts approximately P10 (Storey et al., 2011) and immediately is incorporated into synapses in a process that requires synaptic or sensory activity (Quinlan et al., 1999a; Barria and Malinow, 2002), and it is also induced during synaptic potentiation using well-established LTP protocols (Bellone and Nicoll, 2007).

We hypothesize that the synaptic incorporation of GluN2A-containing NMDARs is dependent on the prior removal of GluN2B-containing receptors. To test this, we used an electrophysiologically tagged GluN2A-containing NMDARs that allowed us to functionally quantify its incorporation into synapses (Barria and Malinow, 2002).

In brief, GluN2A was coexpressed with a mutant form of GluN1 (GluN1 N598R) which eliminates both the normal Mg^{2+} blockade of NMDARs observed at resting membrane potentials and their Ca2+ permeability (Burnashev et al., 1992; Single et al., 2000). It is important to note that expression of GluN1 N598R alone does not lead to functional receptors with endogenous GluN2 subunits, as it remains intracellular, and its currents are not detectable in neurons transfected only with this mutant. However, when coexpressed with recombinant GluN2 subunits, it does form functional receptors, enabling the study of their trafficking and regulation (Huh and Wenthold, 1999; Barria and Malinow, 2002; Prybylowski et al., 2002). Although these previous observations do not explain why recombinant GluN1 does not form functional receptors with endogenous GluN2 subunits, they reinforce the utility of the GluN1 N598R mutant for studying GluN2 subunit trafficking.

Both subunits were optically tagged with GFP to identify transfected CA1 neurons in the slice. In transfected cells, EPSCs evoked at −60 mV exhibit a fast component due to the activation of endogenous AMPARs and a slow component that reflects the activation of recombinant NMDARs, as previously described (Barria and Malinow, 2002). A synaptic incorporation index was calculated by measuring the late component of the EPSC, which occurs 150–200 ms after the stimulus artifact and reflects the synaptic activation of recombinant NMDARs (Fig. 3, gray area on sample traces). This measurement was then normalized to the peak amplitude of the fast component, which reflects the activation of endogenous AMPARs.

We recorded EPSCs at −60 mV in control cells transfected with electrophysiologically tagged GluN2A receptors. As illustrated in Figure 3*A*, a late current indicative of the synaptic incorporation of recombinant GluN2A-containing NMDARs is observed. However, in cells coexpressing the YEKL peptide, which blocks synaptic removal of GluN2B, this current was absent, suggesting that recombinant GluN2A-containing NMDARs were not incorporated into synapses. In contrast, GluN2A-containing NMDARs were normally incorporated into synapses in cells coexpressing the control peptide (Fig. 3*A*).

We also measured the synaptic incorporation of electrophysiologically tagged GluN2B-containing receptors in a similar manner. We found that the YEKL peptide had no effect on the incorporation of recombinant GluN2B-containing receptors, consistent with previous reports indicating that forward trafficking or synaptic incorporation of GluN2B is independent of synaptic activity (Fig. 3*B*; Barria and Malinow, 2002).

These experiments suggest that the internalization of GluN2B, likely induced by the normal synaptic activity that occurs in the cultured organotypic slices during the expression

←

the presence of 2 µM NBQX from CA1 transfected and control neurons recorded as pairs ($n = 12$ pairs). Control peptide was transfected using biolistic and expressed for 2–3 d. Black dot is average ± SEM. ***E***, Top, Sample EPSC traces from a control neuron (gray trace) and a neuron expressing control peptide (black trace). Calibration: 50 ms and 50 pA. Bottom, Peak amplitude of NMDAR-mediated EPSCs from paired recordings normalized to the amplitude of the control nontransfected (NT) neuron. Statistical significance was determined using Wilcoxon matched pairs test ($p = 0.3203$). ***F***, Top, Sample EPSC traces normalized to peak amplitude from a control neuron (gray trace) and a neuron expressing control peptide (black trace). Calibration: 50 ms. Bottom, Weighted tau of NMDAR EPSCs from control nontransfected (NT) neurons and neurons expressing control peptide. Statistical significance was determined using Wilcoxon matched pairs test ($p = 0.5693$). ***G***, Optical detection of surface GluN2B. Top, Sample images of a cultured neuron coexpressing GluN2B-SEP, GluN1, and either YEKL peptide or control peptide before (t_0) and after (t_5) glutamate addition to the bath. Bottom, Quantification of GluN2B-SEP fluorescence in the cell body and proximal dendrites of neurons. Control neurons express only GluN2B-SEP and GluN1. Scale bar, 10 µm.

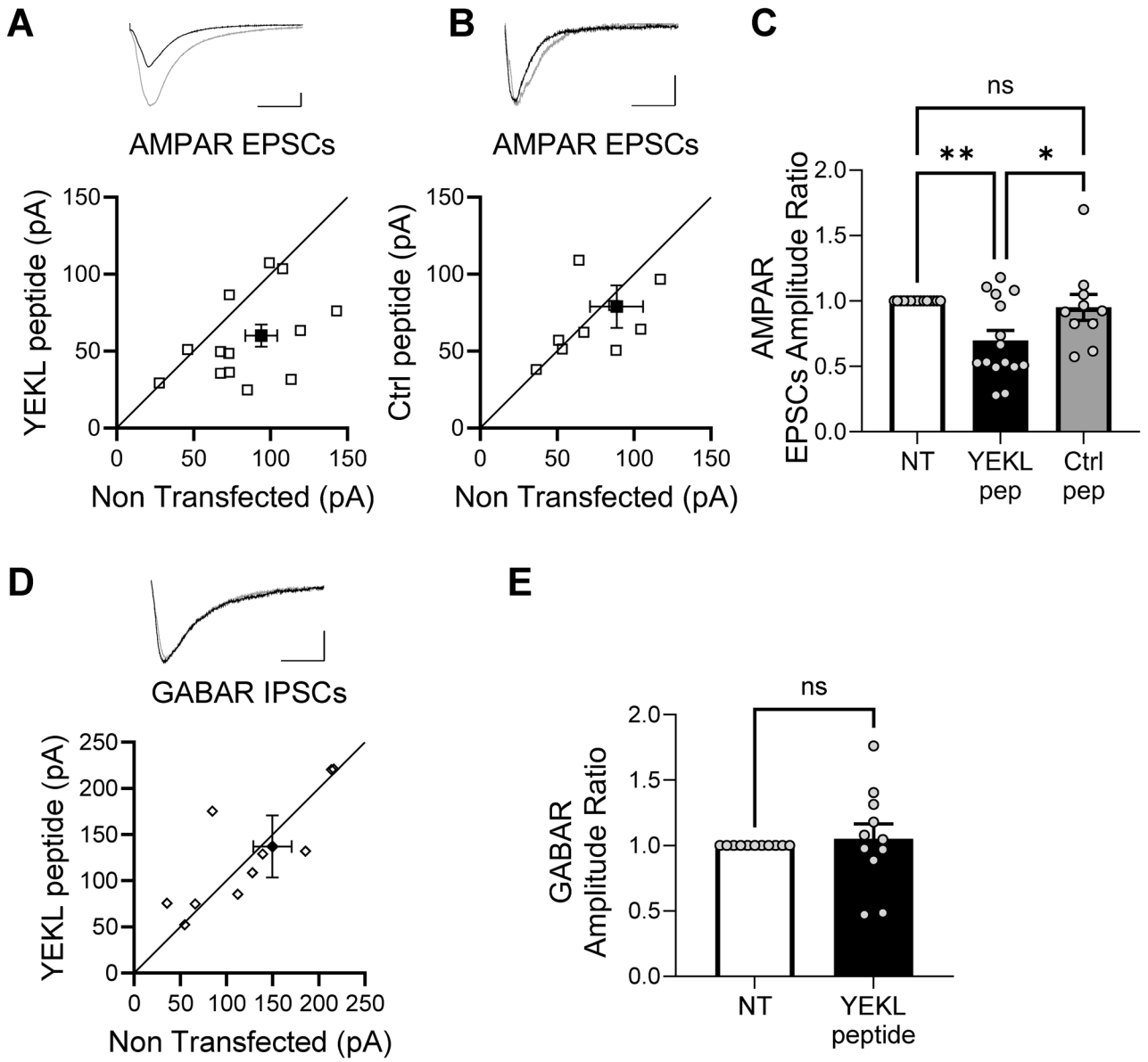

Figure 2. Effect of YEKL peptide on AMPAR-mediated synaptic transmission. ***A***, ***B***, Top, Sample traces of transfected cell and adjacent nontransfected cell recorded as a pair. Bottom, Peak amplitude of paired recordings of AMPAR-mediated EPSCs recorded at −60 mV from CA1 neurons expressing either YEKL peptide (***A***, $n = 15$ pairs) or the control peptide (***B***, $n = 10$ pairs) and an adjacent nontransfected cell (NT). Black square is average ± SEM. ***C***, Peak amplitude of AMPAR-mediated EPSCs from paired recordings of transfected neurons as indicated normalized to the amplitude of the control nontransfected (NT) neuron. Statistical significance was determined using one-way ANOVA ($F = 6.578$; $p = 0.0036$) followed by Tukey's multiple-comparison test (***$p = 0.0009$; *$p = 0.0363$). ***D***, Top, Sample traces of paired recordings of neurons transfected with YEKL peptide and control nontransfected (NT) neurons. Evoked inhibitory postsynaptic currents (IPSCs) were recorded in the presence of 100 µM APV and 2 µM NBQX ($n = 11$ pairs). Optically tagged YEKL peptide was transfected using biolistic and expressed for 2–3 d. Black dot is average ± SEM. ***E***, Peak amplitude of IPSCs from paired recordings normalized to the amplitude of the control nontransfected (NT) neuron. Statistical significance was determined using Wilcoxon matched pairs test ($p = 0.6377$).

period, is required for the synaptic incorporation of recombinant GluN2A. Alternatively, the YEKL peptide could inhibit the lateral diffusion of GluN2B-containing receptors in response to synaptic activity (Gambrill et al., 2011; Dupuis et al., 2014; McQuate and Barria, 2020), a step potentially necessary for clathrin-mediated endocytosis. In this scenario, the requirement for GluN2B to clear from the synapse to allow the incorporation of GluN2A-containing receptors would still exist.

Requirements for synaptic incorporation of recombinant GluN2A-containing receptors

To better understand the synaptic incorporation of GluN2A-containing NMDARs in response to a more defined pattern of synaptic activity, we once again utilized electrophysiologically tagged GluN2A-containing receptors to monitor their synaptic incorporation in real time.

Organotypic hippocampal slices, cultured for 3–5 d, were cotransfected with GluN1 N598R and GluN2A. Subsequently, he slices were cultured for an additional 3 d in the presence of 100 µM APV. This treatment was employed to allow for the expression of the receptor without its synaptic incorporation, as synaptic activity is required for the incorporation of GluN2A into synapses (Barria and Malinow, 2002; Storey et al., 2011).

We recorded evoked EPSCs from CA1 pyramidal cells expressing recombinant NMDARs while holding the membrane potential at −70 mV. Schaffer collaterals were stimulated at a

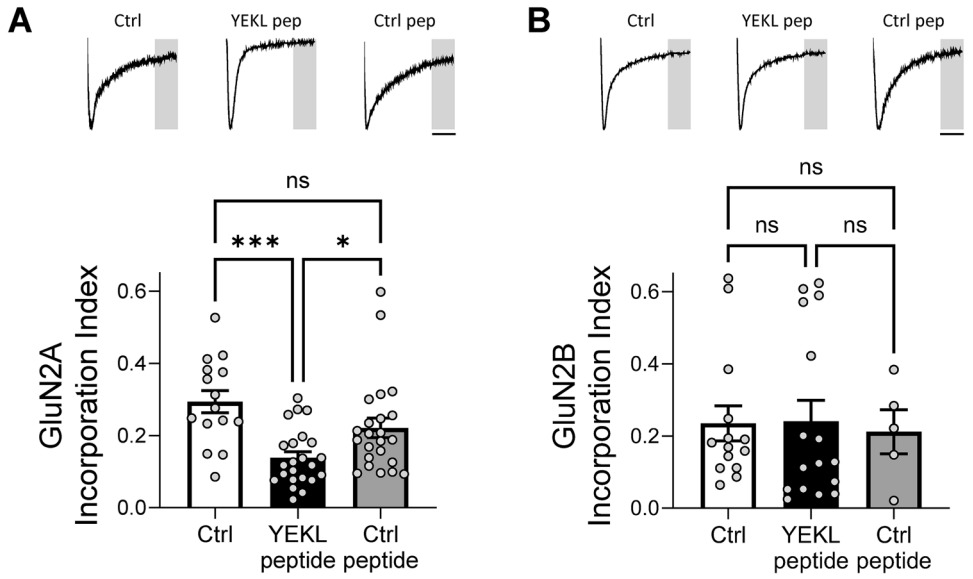

Figure 3. Synaptic incorporation of recombinant GluN2A-containing receptors. ***A***, Top, Sample traces from EPSCs recorded at −70 mV from CA1 neurons cotransfected with GFP-tagged NMDAR subunits GluN2A and GluN1 N598R (left trace) and either YEKL peptide (middle trace) or control peptide (right trace). Calibration: 50 ms. Bottom, GluN2A incorporation index from cells as indicated measured as the average current 150 ms after the stimulus artifact (gray area) normalized to the peak amplitude occurring shortly after the stimulus artifact. Statistical significance was determined using one-way ANOVA ($F = 7.812$; $p = 0.0010$) followed by Tukey's multiple-comparisons test (**$p = 0.0041$; *$p = 0.0364$). Control cells $n = 15$, cells coexpressing YEKL peptide and control peptide $n = 23$ each. ***B***, Top, Sample EPSCs recorded at −70 mV from CA1 neurons cotransfected with GFP-tagged NMDAR subunits GluN2B and GluN1 N598R (left trace) and either YEKL peptide (middle trace) or control peptide (right trace). Calibration: 50 ms. Bottom, GluN2B incorporation index from cells as indicated and measured as in ***A***. Statistical significance was determined using one-way ANOVA ($F = 0.1355$; $p = 0.8737$). Control cells $n = 14$, cells coexpressing YEKL peptide $n = 16$, and cells coexpressing control peptide $n = 5$.

frequency of 0.3 Hz, and the amplitude of the fast component reflecting AMPAR-mediated current was recorded (Fig. 4*A*,*B*). At this point, no current is observed in the time window 150 ms after the stimulus artifact, indicating that recombinant GluN2A receptors have not been incorporated into synapses (Fig. 4*A*,*C*, before pairing traces). Subsequently, synaptic potentiation was induced using a pairing protocol consisting of 3 Hz stimulation for 2 min, with the membrane potential held at 0 mV (Fig. 4*B*, arrow). Figure 4*B* quantifies the increase in amplitude of AMPAR-mediated responses, a well-documented synaptic potentiation of AMPAR-mediated transmission following this pairing protocol (Barria and Malinow, 2005).

To estimate synaptic incorporation of recombinant GluN2A-containing receptors, we measured the late component at 150–200 ms and normalized that value to the peak amplitude of the fast component (Fig. 4*C*, gray area). Before pairing, no recombinant GluN2A-mediated current is observed as expected because APV had blocked the incorporation of recombinant GluN2A (Fig. 4*C*, before pairing). Following the pairing protocol, a rapid increase in this current is clearly observed, indicating rapid incorporation of recombinant GluN2A-containing receptors (Fig. 4*D*).

These experiments establish that a widely used LTP-inducing protocol, in addition to augmenting AMPAR-mediated synaptic transmission, also drives synaptic incorporation of GluN2A-containing receptors.

Next, we employed this approach to examine whether synaptic activity alone, specifically glutamate release from presynaptic terminals, was adequate to acutely drive the synaptic incorporation of recombinant GluN2A, or if postsynaptic Ca^{2+} influx was necessary for this process.

In CA1 pyramidal cells expressing recombinant GluN2A-containing receptors, following a baseline period, we increased the stimulation rate to 3 Hz for 2 min while maintaining the cell at −70 mV to prevent the activation of endogenous NMDARs. Despite this brief period of increased activity, no significant changes in the late component of EPSCs were observed (Fig. 4*E*), indicating that this level of activity was insufficient to drive the synaptic incorporation of recombinant GluN2A. This suggests that current flowing through existing endogenous synaptic NMDARs is necessary.

To confirm that calcium influx is indeed a requirement for GluN2A synaptic incorporation, we repeated the experiment with a calcium chelator in the pipette (10 mM BAPTA). The LTP-inducing protocol used previously failed to induce potentiation of the AMPAR-mediated synaptic transmission, as expected. Importantly, it also failed to induce synaptic incorporation of electrophysiologically tagged GluN2A-containing receptors (Fig. 4*F*).

Figure 4, *G* and *H*, depicts the quantification of the potentiation of AMPAR-mediated and recombinant NMDAR-mediated EPSCs, respectively, observed after 25–30 min of the pairing protocol under different conditions as indicated. These experiments indicate that synaptic activity, through the activation of existing synaptic NMDARs and subsequent postsynaptic calcium influx, is necessary for GluN2A synaptic incorporation.

Taken together, these experiments suggest that the synaptic incorporation of GluN2A-containing receptors and the potentiation of AMPAR-mediated synaptic transmission are interconnected processes. Indeed, a positive correlation is observed when the potentiation of AMPAR-mediated synaptic transmission is plotted against the potentiation of the late component mediated by the newly inserted GluN2A receptors (Fig. 4*I*).

Removal of GluN2B is required for rapid synaptic incorporation of GluN2A

After directly examining the requirements for inducing the rapid incorporation of electrophysiologically tagged GluN2A-containing receptors into synapses, our next question was whether blockade of synaptic activity-induced GluN2B removal is necessary.

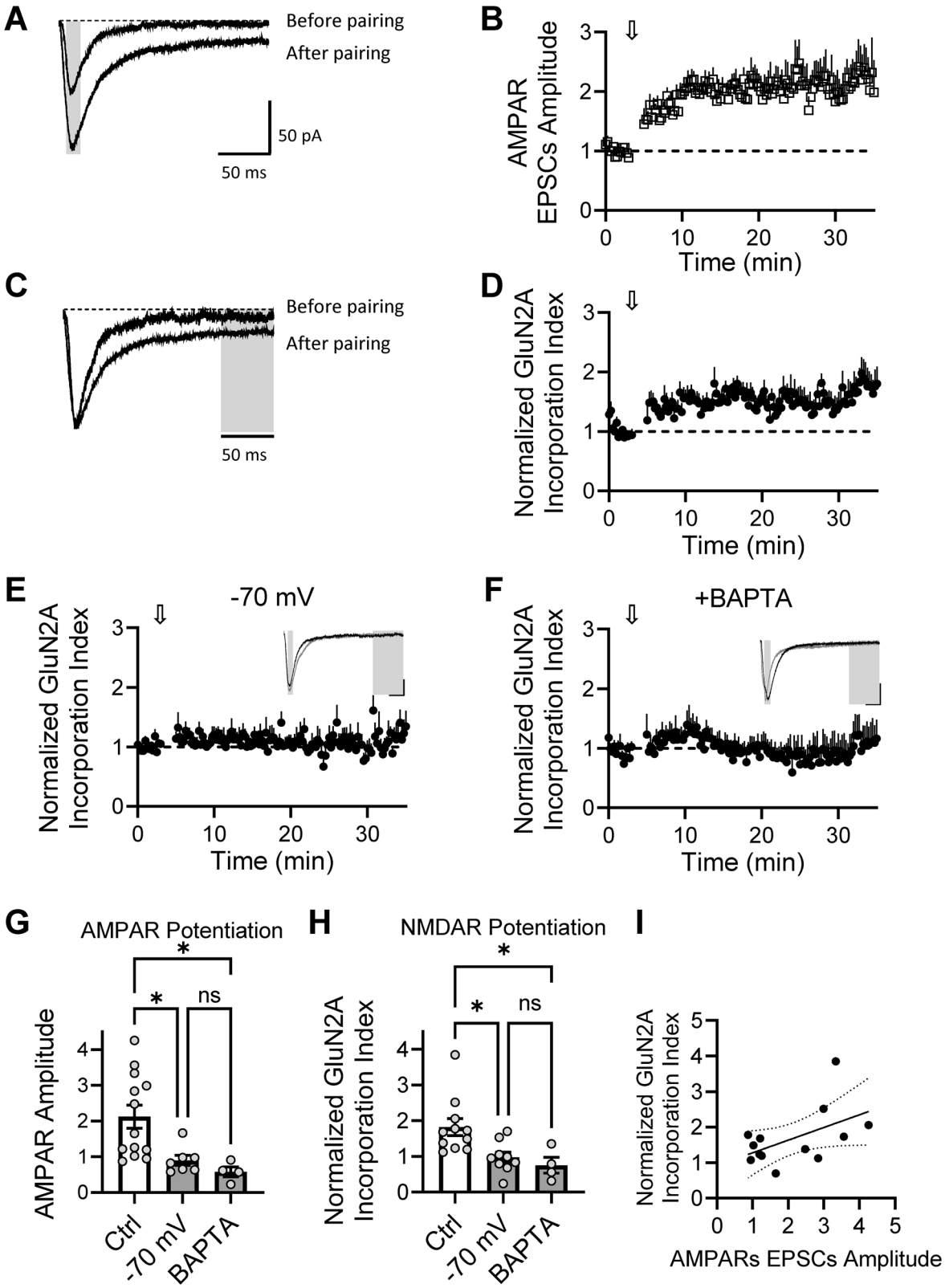

Figure 4. Rapid synaptic incorporation of GluN2A-containing receptors. ***A***, Sample traces of evoked excitatory postsynaptic currents (EPSCs) recorded at −70 mV from a CA1 neuron cotransfected with GFP-tagged NMDAR subunits GluN2A and GluN1 N598R. The traces show responses during baseline (before a pairing protocol) and 20 min after potentiation, which was induced by a 2 min, 3 Hz stimulation while holding the cell at 0 mV. ***B***, Peak amplitude of EPSCs from CA1 neurons as in ***A***, with the gray area indicating the AMPAR-mediated component of the EPSCs. The arrow indicates the point where the pairing protocol was applied to induce potentiation ($n = 15$). ***C***, Sample traces as in ***A*** normalized to the peak amplitude of the response. The recombinant NMDAR current is quantified 150–200 ms after the stimulus artifact (gray area). ***D***, Amplitude of the current carried by GluN2A-containing recombinant NMDARs over time, normalized to the average of baseline measurements. The arrow indicates the application of the pairing protocol, which involves 2 min of 3 Hz stimulation while holding the cell at 0 mV. ***E***, Amplitude of the current carried by GluN2A-containing recombinant NMDARs normalized to the average of baseline measurements. In this experiment the pairing protocol consisted of 2 min of 3 Hz stimulation while holding the cell at −70 mV ($n = 23$). Inset, Sample traces of EPSCs before (gray) and after (black) pairing protocol. Gray areas indicate where the AMPAR-mediated EPSC and the GluN2A

We coexpressed electrophysiologically tagged GluN2A receptors with either the YEKL peptide or the control peptide in organotypic slices. As previously, slices were maintained in 100 μM APV during the expression period (3 d in culture) to prevent the incorporation of recombinant GluN2A into synapses.

Figure 5, *A* and *B*, shows the late component of evoked synaptic responses, which represents the amount of recombinant GluN2A that has incorporated into synapses. After 3–5 min of baseline recording, a pairing protocol of 3 Hz stimulation for 2 min with the cell voltage clamped at 0 mV was applied. Neurons coexpressing the control peptide exhibited a rapid incorporation of recombinant GluN2A-containing receptors, as shown in Figure 5*A*. In contrast, cells coexpressing the YEKL peptide did not show this incorporation, as illustrated in Figure 5*B*. This result further supports the notion that GluN2B internalization is necessary for the synaptic incorporation of GluN2A.

Interestingly, expression of the YEKL peptide also prevented potentiation of AMPAR-mediated synaptic transmission (Fig. 5*E*,*F*), adding to evidence suggesting that AMPAR potentiation is linked to the incorporation of GluN2A into the synapse. The control peptide had no effect on the synaptic potentiation of AMPAR (Fig. 5*D*,*F*).

Acute blockade on GluN2B internalization also prevents GluN2A synaptic incorporation and AMPAR potentiation

We were concerned that prolonged blockade of GluN2B removal via expression of the YEKL peptide could potentially lead to a misinterpretation of our results. To address this concern, we next examined the effects of acute blockade of GluN2B removal on the rapid synaptic incorporation of GluN2A and AMPAR potentiation.

We used an antennapedia fusion peptide containing the YEKL domain of the GluN2B carboxy-tail (Ant-YEKL). The antennapedia sequence renders our YEKL domain peptide membrane permeable, allowing for its brief application directly to the slice culture media before recordings (Fink et al., 2003; Illario et al., 2003; Schmitt et al., 2004; Sanhueza et al., 2007). Additionally, we developed a control antennapedia fusion peptide named Ant-AEKL, which incorporated the same GluN2B C-tail sequence as Ant-YEKL but with the tyrosine (Y) replaced by an alanine (A), thus preventing this peptide from binding to AP-2 (Prybylowski et al., 2005).

Cultured organotypic hippocampal slices were transfected with electrophysiologically tagged GluN2A-containing receptors and cultured with 100 μM APV to prevent synaptic incorporation during the expression period due to spontaneous activity in the slice (Barria and Malinow, 2002).

The slices were treated with either 5 μM of Ant-YEKL or Ant-AEKL for 2 h before recording evoked currents from transfected CA1 pyramidal neurons, while maintaining the cell at −70 mV. As before, we measured the fast component of the evoked EPSCs, indicative of AMPA-mediated transmission, and the late component of the EPSC, indicative of electrophysiologically tagged GluN2A presence at synapses.

After establishing a stable baseline for 3–5 min, we applied a pairing protocol consisting of 3 Hz stimulation while holding the cell at a voltage of 0 mV. In slices treated with the control Ant-AEKL peptide, we observed rapid synaptic incorporation of recombinant GluN2A-containing receptors (Fig. 6*A*), along with the expected potentiation of AMPAR-mediated EPSCs (Fig. 6*D*).

In contrast, in slices treated with the Ant-YEKL peptide synaptic incorporation of recombinant GluN2A-containing receptors was prevented (Fig. 6*B*,*C*) as well as potentiation of AMPAR-mediated currents (Fig. 6*E*,*F*).

We also used a pharmacological approach to block activity-dependent internalization of GluN2B-containing receptors. We used the casein kinase II inhibitor, TBB. Phosphorylation of GluN2B by casein kinase II has been shown to be a critical step in triggering activity-dependent removal of GluN2B from the synapse (Sanz-Clemente et al., 2010).

Hippocampal slices expressing electrophysiologically tagged GluN2A receptors were treated with 10 μM TBB for 2 h before recording. As before, slices were cultured with 100 μM APV to prevent incorporation of GluN2A during the expression period.

In Figure 7*A*, consistent with the outcomes observed with the expression of the YEKL peptide (Figs. 3, 5) and treatment with Ant-YEKL peptide (Fig. 6), pharmacological inhibition of GluN2B synaptic removal impeded the rapid incorporation of recombinant GluN2A induced by the pairing protocol. Moreover, the prevention of GluN2A incorporation coincided with the absence of potentiation in the AMPAR-mediated component of the EPSC, aligning with the findings from other experiments (Fig. 7*B*).

Together, these experiments indicate that the removal of GluN2B receptors in an activity-dependent manner is necessary to allow for the synaptic incorporation of GluN2A receptors. Additionally, they suggest that the potentiation of AMPAR-mediated synaptic transmission is linked to the synaptic incorporation of GluN2A-containing NMDA receptors.

Discussion

The expression of glutamate receptors at synaptic sites follows a well-orchestrated choreography, characterized by specific temporal and regional patterns in the production of the various subunits that make up both AMPA-type and NMDA-type receptors. These different subunits endow the ion channels with distinct biophysical properties and determine their capacity to interact with specific postsynaptic scaffolding and signaling proteins (Dingledine et al., 1999; Traynelis et al., 2010; Hansen et al., 2021).

The precise modulation of synaptic currents and the interactions with postsynaptic proteins play a crucial role in regulating synaptic plasticity (Barria and Malinow, 2005; Zhou et al., 2007), which is essential for the proper selection of synaptic contacts and the development of neuronal circuits. Consequently, disruptions in the expression and synaptic incorporation of glutamate receptor subunits during early synaptogenesis can lead to aberrant neural wiring, potentially manifesting later in life as

←

were measured. ***F***, Amplitude of the current carried by GluN2A-containing recombinant NMDARs over time, normalized to the average of baseline measurements from CA1 neurons. Recordings were conducted with internal solution containing BAPTA. The arrow indicates the application of the pairing protocol, which involves 2 min of 3 Hz stimulation while holding the cell at 0 mV ($n = 12$). Inset, Sample traces of EPSCs before (gray) and after (black) pairing protocol. Gray areas indicate where the AMPAR-mediated EPSC and the GluN2A were measured. ***G***, ***H***, Quantification of potentiation 30–35 min after the start of the experiment, measuring the AMPAR-mediated component of the EPSC (***G***) and the late component of the EPSC resulting from the synaptic expression of GluN2A-containing recombinant NMDARs (***H***). Statistical significance was determined using one-way ANOVA (AMPAR potentiation $F = 6.645$ and $p = 0.0058$; NMDAR potentiation $F = 6.452$ and $p = 0.0065$) followed by Tukey's multiple-comparisons test. Asterisk $p < 0.05$. ***I***, Correlation between AMPAR potentiation after pairing protocol and synaptic incorporation of GluN2A-containing recombinant NMDARs. Line is linear regression fit with 95% confidence interval.

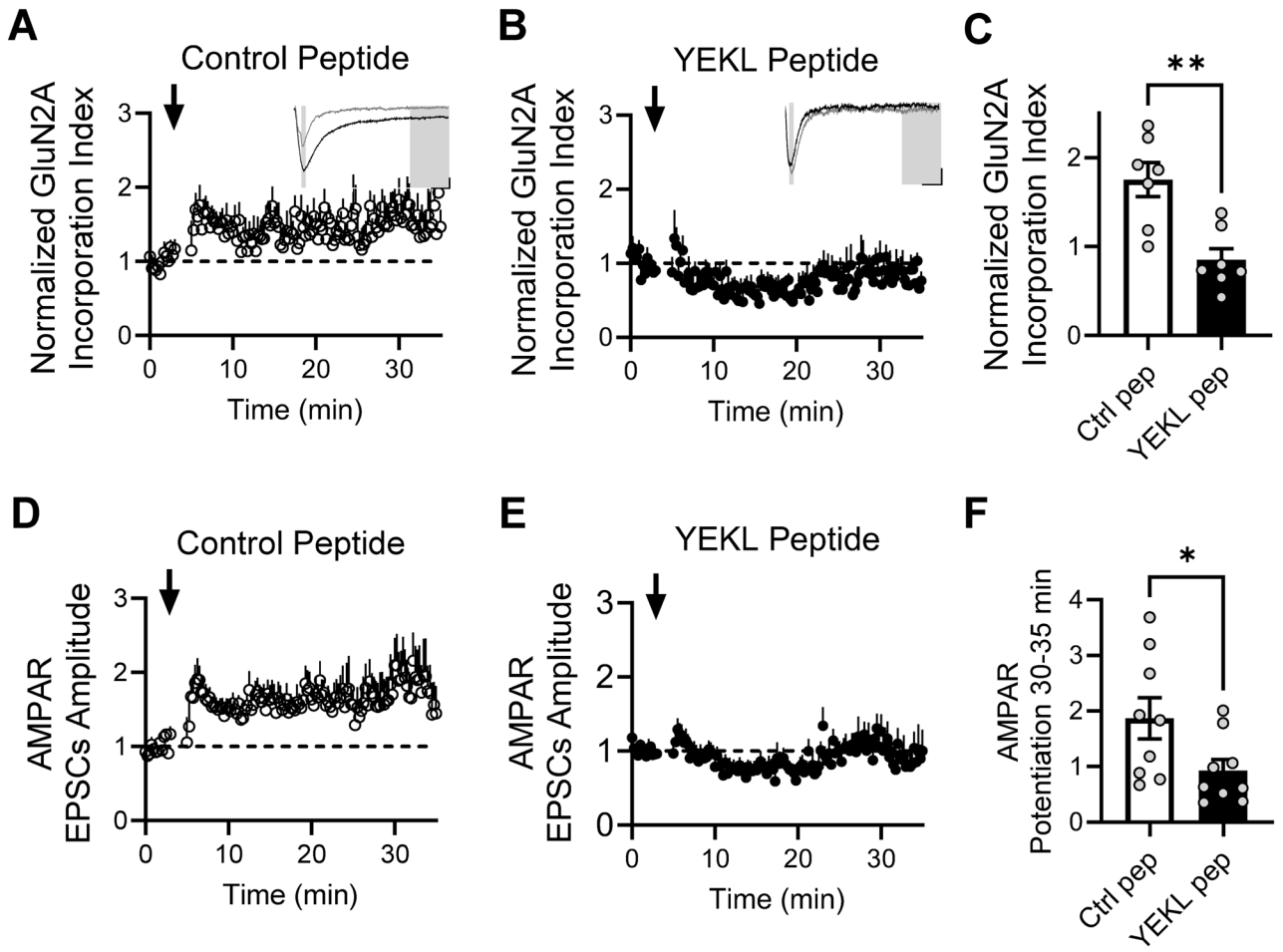

Figure 5. Synaptic incorporation of GluN2A-containing receptors while blocking internalization of GluN2B. ***A***, Amplitude of the current carried by GluN2A-containing recombinant NMDARs over time in CA1 neurons cotransfected with GFP-tagged NMDAR subunits GluN2A and GluN1 N598R, along with the control peptide ($n = 14$). EPSCs were recorded at −70 mV and the GluN2A current measured 150 ms after the stimulus artifact. The arrow indicates the induction of synaptic potentiation through a pairing protocol, which consists of 2 min, 3 Hz stimulation while holding the cell at 0 mV. GluN2A incorporation index is normalized to baseline measurements. Inset, Sample traces of EPSCs before (gray) and after (black) pairing protocol. Gray areas indicate where the AMPAR-mediated EPSC and the GluN2A were measured. ***B***, Amplitude of the current carried by GluN2A-containing recombinant NMDARs over time in CA1 neurons cotransfected with GFP-tagged NMDAR subunits GluN2A and GluN1 N598R, along with the YEKL peptide ($n = 10$). EPSCs were recorded at −70 mV and the GluN2A current measured 150 ms after the stimulus artifact. The arrow indicates the induction of synaptic potentiation through a pairing protocol, which consists of 2 min, 3 Hz stimulation while holding the cell at 0 mV. GluN2A incorporation index is normalized to baseline measurements. Inset, sample traces of EPSCs before (gray) and after (black) pairing protocol. Gray areas indicate where the AMPAR-mediated EPSC and the GluN2A were measured. ***C***, Quantification of recombinant GluN2A synaptic incorporation 30–35 min after the start of the experiment for neurons coexpressing either the control peptide or the YEKL peptide. Statistical significance was determined using Mann–Whitney test ($p = 0.0070$). ***D***, Peak amplitude of EPSCs recorded at −70 mV, representing the AMPAR component of the EPSC, in CA1 neurons as in ***A***, i.e., expressing the control peptide. ***E***, Peak amplitude of EPSCs recorded at −70 mV, representing the AMPAR component of the EPSC, in CA1 neurons as in ***B***, i.e., expressing YEKL peptide. ***F***, Quantification of AMPAR-mediated synaptic transmission 30–35 min after start of the experiment in neurons expressing either the control peptide or the YEKL peptide. Statistical significance was determined using Mann–Whitney test ($p = 0.0315$).

cognitive disorders such as fragile X syndrome or schizophrenia (Banke and Barria, 2020; Banke et al., 2024).

Of particular importance is the switch in GluN2 subunits of synaptic NMDARs. Receptors containing either GluN2A or GluN2B follow different paths to reach synapses and are also removed in a different manner from them. While GluN2B-containing receptors can reach synapses independently of synaptic activity, GluN2A-containing receptors require a certain level of synaptic activity for their incorporation into synapses (Barria and Malinow, 2002). GluN2B is often expressed extrasynaptically, where it has a high diffusion coefficient (Groc et al., 2006; Kellermayer et al., 2018), allowing it to be incorporated into synapses through lateral diffusion (Gambrill et al., 2011; Dupuis et al., 2014; McQuate and Barria, 2020). This same mechanism allows GluN2B to leave synapses, though it can also be internalized via clathrin-dependent endocytosis through a YEKL motif in its carboxy-terminal domain that interacts with the AP2 complex (Lavezzari et al., 2003, 2004). Additionally, GluN2B has been found to increase spine and filopodia motility (Gambrill and Barria, 2011). In contrast, GluN2A-containing receptors seem to be trafficked directly to dendritic spines—the primary sites of synaptic contact in most excitatory neurons. They tend to accumulate in these locations if the binding of glutamate to pre-existing synaptic receptors is blocked, which prevents their synaptic incorporation (Barria and Malinow, 2002). Once at the synapse, GluN2A-containing receptors are generally more stable, and it has been proposed that they confer stability to synapses and spine structures (Foster et al., 2010; Gambrill and Barria, 2011).

Changes in the decay kinetics of isolated NMDAR-mediated EPSCs, along with sensitivity to ifenprodil, a specific noncompetitive antagonist of GluN2B, clearly indicates that as synapses

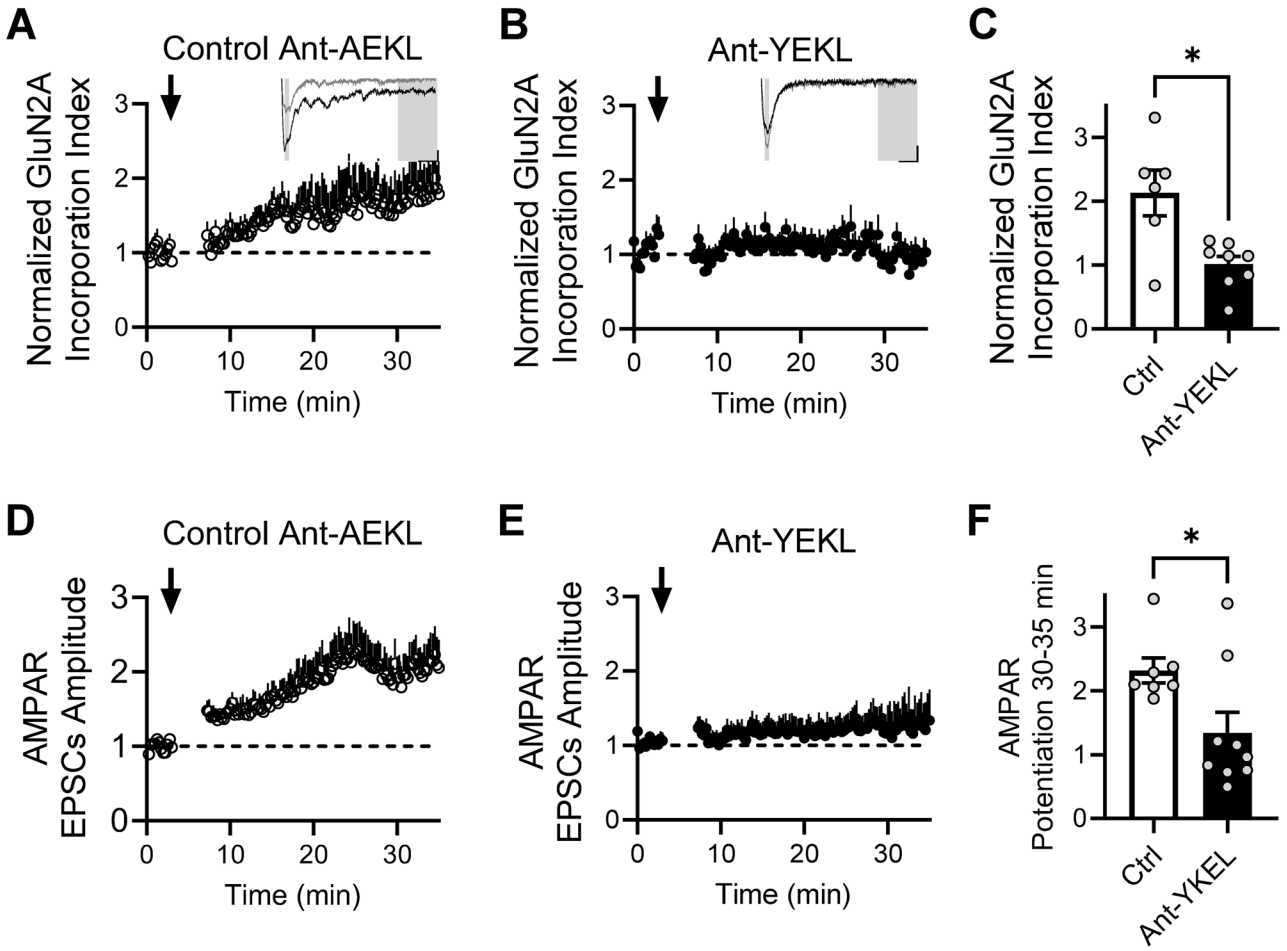

Figure 6. Rapid blockade of GluN2B internalization and its effect on GluN2A synaptic incorporation. ***A***, Amplitude of the current carried by GluN2A-containing recombinant NMDARs over time in CA1 neurons cotransfected with GFP-tagged NMDAR subunits GluN2A and GluN1 N598R. GluN2A incorporation index is normalized to baseline measurements. Slices were incubated with the control antennapedia peptide Ant-AEKL for 2 h before the experiment ($n = 9$). EPSCs were recorded at −70 mV and the recombinant GluN2A current measured 150 ms after the stimulus artifact. The arrow indicates the induction of synaptic potentiation through a pairing protocol, which consists of 2 min, 3 Hz stimulation while holding the cell at 0 mV. Inset, Sample traces of EPSCs before (gray) and after (black) pairing protocol. Gray areas indicate where the AMPAR-mediated EPSC and the GluN2A were measured. ***B***, Amplitude of the current carried by GluN2A-containing recombinant NMDARs over time in CA1 neurons cotransfected with GFP-tagged NMDAR subunits GluN2A and GluN1 N598R. GluN2A incorporation index is normalized to baseline measurements. Slices were incubated with the antennapedia peptide Ant-YEKL for 2 h before the experiment ($n = 9$). EPSCs were recorded at −70 mV and the GluN2A current measured 150 ms after the stimulus artifact. The arrow indicates the induction of synaptic potentiation through a pairing protocol, which consists of 2 min, 3 Hz stimulation while holding the cell at 0 mV. Inset, Sample traces of EPSCs before (gray) and after (black) pairing protocol. Gray areas indicate where the AMPAR-mediated EPSC and the GluN2A were measured. ***C***, Quantification of recombinant GluN2A synaptic incorporation 30–35 min after the start of the experiment for neurons treated with either the control Ant-AEKL peptide or the Ant-YEKL peptide. Statistical significance was determined using Mann–Whitney test ($p = 0.0293$). ***D***, Peak amplitude of EPSCs recorded at −70 mV, representing the AMPAR component of the EPSC, in CA1 neurons coexpressing GFP-tagged NMDAR subunits GluN2A and GluN1 N598R and treated with control antennapedia peptide Ant-AEKL. ***E***, Peak amplitude of EPSCs recorded at −70 mV, representing the AMPAR component of the EPSC, in CA1 neurons coexpressing GFP-tagged NMDAR subunits GluN2A and GluN1 N598R and treated with antennapedia peptide Ant-YEKL. ***F***, Quantification of AMPAR-mediated synaptic transmission 30–35 min after the start of the experiment for neurons treated with either the control Ant-AEKL peptide or the Ant-YEKL peptide. Statistical significance was determined using Mann–Whitney test ($p = 0.0418$).

mature, the ratio of GluN2B to GluN2A decreases. However, it remains unclear whether this involves a direct one-to-one exchange of GluN2B for GluN2A, or if GluN2B leaves synapses through simple diffusion or an activity-dependent mechanism involving receptor endocytosis. Since synaptic incorporation of GluN2A requires glutamate binding to pre-existing NMDARs, it has been proposed that clathrin-mediated removal of GluN2B creates a synaptic spot for GluN2A insertion. The observation that LTP at hippocampal glutamatergic synapses results in faster decay kinetics of NMDAR-mediated EPSCs without a change in their peak amplitude (Bellone and Nicoll, 2007) also supports the idea of a one-to-one exchange between GluN2B and GluN2A.

Our results directly tested this hypothesis by blocking the clathrin-dependent removal of GluN2B-containing receptors. By blocking the endocytosis of GluN2B-containing NMDARs through the expression of the YEKL peptide in CA1 neurons, and measuring the synaptic incorporation of recombinant GluN2A, which is not inhibited by Mg^{2+}, we demonstrate that these two processes are directly linked, supporting the hypothesis that the removal of GluN2B is necessary for the incorporation of GluN2A at synapses.

The issue of whether trimeric receptors, composed of two GluN1 subunits alongside one GluN2A and one GluN2B, behave similarly to NMDARs with only one type of GluN2 subunit presents a complex challenge. Specifically, it remains unclear whether triheteromeric receptors are internalized or dispersed from synaptic sites in the same manner as diheteromeric GluN1/GluN2B receptors, require the removal of GluN2B for synaptic insertion, or if they can laterally diffuse into synapses like diheteromeric GluN1/GluN2B.

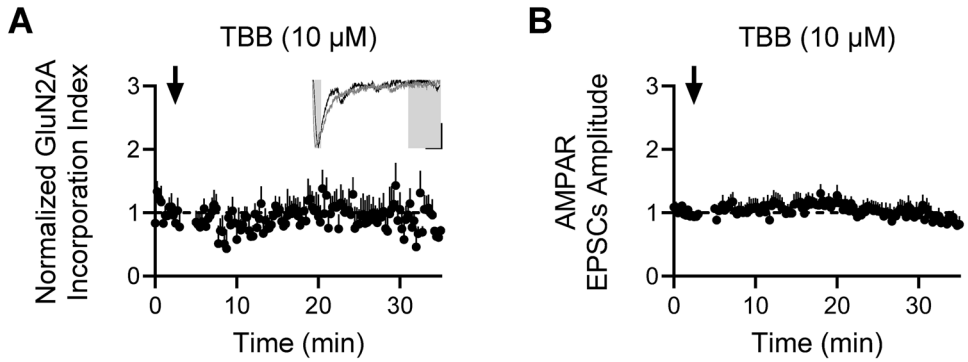

Figure 7. Inhibition of casein kinase II and its effect on GluN2A synaptic incorporation. ***A***, Amplitude of the current carried by GluN2A-containing recombinant NMDARs over time in CA1 neurons cotransfected with GFP-tagged NMDAR subunits GluN2A and GluN1 N598R. Slices were incubated with TBB, a casein kinase II inhibitor, 2 h before the experiment ($n = 8$). EPSCs were recorded at −70 mV and the GluN2A current measured 150 ms after the stimulus artifact. The arrow indicates the induction of synaptic potentiation through a pairing protocol, which consists of 2 min, 3 Hz stimulation while holding the cell at 0 mV. GluN2A incorporation index is normalized to baseline measurements. Inset, Sample traces of EPSCs before (gray) and after (black) pairing protocol. Gray areas indicate where the AMPAR-mediated EPSC and the GluN2A were measured. ***B***, Peak amplitude of EPSCs recorded at −70 mV, representing the AMPAR component of the EPSC, in CA1 neurons coexpressing GFP-tagged NMDAR subunits GluN2A and GluN1 N598R, and treated with TBB for 2 h before the experiment.

By employing a protocol that enables the expression of Mg^{2+}-insensitive GluN2A-containing receptors while preventing their synaptic incorporation (Barria and Malinow, 2002), we were able to examine specific conditions necessary for GluN2A's synaptic incorporation in real time.

Understanding the conditions required for GluN2A synaptic incorporation is crucial, as it has been observed that in hippocampal slices treated with tetrodotoxin (TTX) for 2–3 d, which blocks synaptic activity but not spontaneous neurotransmitter release, GluN2A is still incorporated into synapses. This suggests a mechanism that removes existing NMDARs without activating their ion channels and, therefore, operates in a Ca^{2+}-independent manner (Barria and Malinow, 2002).

Our results demonstrate that the rapid synaptic incorporation of GluN2A induced by a commonly used LTP protocol requires postsynaptic Ca^{2+}, indicating that mere glutamate release is not enough to trigger the switch in subunit composition. It is possible that stimulation of pre-existing NMDARs by spontaneous release of glutamate during the 2–3 d of TTX incubation still can produce small Ca^{2+} transients necessary for the incorporation of GluN2A or that a slower activity-independent synaptic incorporation of GluN2A exist.

Notably, interfering with GluN2B internalization—whether by expressing the YEKL peptide or using rapid blockade with Ant-YEKL peptide or TBB—not only prevents the incorporation of recombinant GluN2A into synapses induced by an LTP protocol but also inhibits the potentiation of synaptic currents mediated by AMPARs.

Immobilizing GluN2B-containing receptors on the surface of neurons using antibodies targeting the extracellular domain of GluN2B also inhibits various LTP-inducing protocols, as evidenced by changes in spine volume and electrophysiological recordings (Dupuis et al., 2014). It is possible that altering the surface dynamics of GluN2B-containing receptors also prevents their internalization in response to synaptic activity, thereby supporting the notion that an activity-dependent switch of GluN2 subunits is associated with the synaptic incorporation of AMPA-type glutamate receptors and LTP.

This suggests that LTP not only boosts AMPAR trafficking (Kessels and Malinow, 2009) but also incorporates GluN2A. Such a process could promote synaptic structure stability, as studies suggest that dendritic spines containing GluN2A are more stable than those with GluN2B (Gambrill and Barria, 2011). Currently, it is not fully understood how disruption of GluN2 subunit exchange also impacts the synaptic incorporation of AMPARs in response to LTP-inducing protocols. It has been proposed that AMPARs are sourced from recycling endosomes (Park et al., 2004) and/or through lateral diffusion (Penn et al., 2017) during LTP. The question of whether GluN2A and AMPARs are incorporated from the same intracellular compartments remains open and is an intriguing topic for future research.

These findings shed light on the molecular mechanisms driving the switch from GluN2B to GluN2A in NMDA receptors. They also reveal how functional interactions between various glutamate receptors in the brain may regulate the levels of AMPARs and contribute to synaptic potentiation and stabilization.

References

Akazawa C, Shigemoto R, Bessho Y, Nakanishi S, Mizuno N (1994) Differential expression of five N-methyl-D-aspartate receptor subunit mRNAs in the cerebellum of developing and adult rats. J Comp Neurol 347:150–160.

Al-Hallaq RA, Conrads TP, Veenstra TD, Wenthold RJ (2007) NMDA di-heteromeric receptor populations and associated proteins in rat hippocampus. J Neurosci 27:8334–8343.

Banke TG, Barria A (2020) Transient enhanced GluA2 expression in young hippocampal neurons of a fragile X mouse model. Front Synaptic Neurosci 12:588295.

Banke TG, Traynelis SF, Barria A (2024) Early expression of GluN2A-containing NMDA receptors in a model of fragile X syndrome. J Neurophysiol 131:768–777.

Barria A, Malinow R (2002) Subunit-specific NMDA receptor trafficking to synapses. Neuron 35:345–353.

Barria A, Malinow R (2005) NMDA receptor subunit composition controls synaptic plasticity by regulating binding to CaMKII. Neuron 48:289–301.

Bellone C, Nicoll RA (2007) Rapid bidirectional switching of synaptic NMDA receptors. Neuron 55:779–785.

Burnashev N, Schoepfer R, Monyer H, Ruppersberg JP, Gunther W, Seeburg PH, Sakmann B (1992) Control by asparagine residues of calcium permeability and magnesium blockade in the NMDA receptor. Science 257:1415–1419.

Carmignoto G, Vicini S (1992) Activity-dependent decrease in NMDA receptor responses during development of the visual cortex. Science 258:1007–1011.

Cerpa W, Gambrill A, Inestrosa NC, Barria A (2011) Regulation of NMDA-receptor synaptic transmission by Wnt signaling. J Neurosci 31:9466–9471.

Dingledine R, Borges K, Bowie D, Traynelis SF (1999) The glutamate receptor ion channels. Pharmacol Rev 51:7–61.

Dupuis JP, et al. (2014) Surface dynamics of GluN2B-NMDA receptors controls plasticity of maturing glutamate synapses. EMBO J 33:842–861.

Ewald RC, Van Keuren-Jensen KR, Aizenman CD, Cline HT (2008) Roles of NR2A and NR2B in the development of dendritic arbor morphology in vivo. J Neurosci 28:850–861.
Fink CC, Bayer KU, Myers JW, Ferrell JE Jr, Schulman H, Meyer T (2003) Selective regulation of neurite extension and synapse formation by the beta but not the alpha isoform of CaMKII. Neuron 39:283-297.
Foster KA, McLaughlin N, Edbauer D, Phillips M, Bolton A, Constantine-Paton M, Sheng M (2010) Distinct roles of NR2A and NR2B cytoplasmic tails in long-term potentiation. J Neurosci 30:2676–2685.
Gambrill AC, Barria A (2011) NMDA receptor subunit composition controls synaptogenesis and synapse stabilization. Proc Natl Acad Sci U S A 108: 5855–5860.
Gambrill AC, Storey GP, Barria A (2011) Dynamic regulation of NMDA receptor transmission. J Neurophysiol 105:162–171.
Gray JA, Shi Y, Usui H, During MJ, Sakimura K, Nicoll RA (2011) Distinct modes of AMPA receptor suppression at developing synapses by GluN2A and GluN2B: single-cell NMDA receptor subunit deletion in vivo. Neuron 71:1085–1101.
Groc L, Heine M, Cousins SL, Stephenson FA, Lounis B, Cognet L, Choquet D (2006) NMDA receptor surface mobility depends on NR2A-2B subunits. Proc Natl Acad Sci U S A 103:18769–18774.
Halt AR, Dallapiazza RF, Zhou Y, Stein IS, Qian H, Juntti S, Wojcik S, Brose N, Silva AJ, Hell JW (2012) CaMKII binding to GluN2B is critical during memory consolidation. EMBO J 31:1203–1216.
Hansen KB, et al. (2021) Structure, function, and pharmacology of glutamate receptor ion channels. Pharmacol Rev 73:298–487.
Hayashi T, Thomas GM, Huganir RL (2009) Dual palmitoylation of NR2 subunits regulates NMDA receptor trafficking. Neuron 64:213–226.
Huh KH, Wenthold RJ (1999) Turnover analysis of glutamate receptors identifies a rapidly degraded pool of the N-methyl-D-aspartate receptor subunit, NR1, in cultured cerebellar granule cells. J Biol Chem 274:151–157.
Illario M, Cavallo AL, Bayer KU, Di Matola T, Fenzi G, Rossi G, Vitale M (2003) Calcium/calmodulin-dependent protein kinase II binds to Raf-1 and modulates integrin-stimulated ERK activation. J Biol Chem 278: 45101–45108.
Kellermayer B, et al. (2018) Differential nanoscale topography and functional role of GluN2-NMDA receptor subtypes at glutamatergic synapses. Neuron 100:106–119.e7.
Kessels HW, Malinow R (2009) Synaptic AMPA receptor plasticity and behavior. Neuron 61:340–350.
Kittler JT, Delmas P, Jovanovic JN, Brown DA, Smart TG, Moss SJ (2000) Constitutive endocytosis of GABAA receptors by an association with the adaptin AP2 complex modulates inhibitory synaptic currents in hippocampal neurons. J Neurosci 20:7972–7977.
Kneussel M (2002) Dynamic regulation of GABA(A) receptors at synaptic sites. Brain Res Brain Res Rev 39:74–83.
Kutsuwada T, et al. (1996) Impairment of suckling response, trigeminal neuronal pattern formation, and hippocampal LTD in NMDA receptor epsilon 2 subunit mutant mice. Neuron 16:333–344.
Lavezzari G, McCallum J, Dewey CM, Roche KW (2004) Subunit-specific regulation of NMDA receptor endocytosis. J Neurosci 24:6383–6391.
Lavezzari G, McCallum J, Lee R, Roche KW (2003) Differential binding of the AP-2 adaptor complex and PSD-95 to the C-terminus of the NMDA receptor subunit NR2B regulates surface expression. Neuropharmacology 45: 729–737.
Mattison HA, Hayashi T, Barria A (2012) Palmitoylation at two cysteine clusters on the C-terminus of GluN2A and GluN2B differentially control synaptic targeting of NMDA receptors. PLoS One 7:e49089.
Mayadevi M, Praseeda M, Kumar KS, Omkumar RV (2002) Sequence determinants on the NR2A and NR2B subunits of NMDA receptor responsible for specificity of phosphorylation by CaMKII. Biochim Biophys Acta 1598:40–45.
McQuate A, Barria A (2020) Rapid exchange of synaptic and extrasynaptic NMDA receptors in hippocampal CA1 neurons. J Neurophysiol 123: 1004–1014.
McQuate A, Latorre-Esteves E, Barria A (2017) A Wnt/calcium signaling cascade regulates neuronal excitability and trafficking of NMDARs. Cell Rep 21:60–69.
Monyer H, Burnashev N, Laurie DJ, Sakmann B, Seeburg PH (1994) Developmental and regional expression in the rat brain and functional properties of four NMDA receptors. Neuron 12:529–540.
Omkumar RV, Kiely MJ, Rosenstein AJ, Min KT, Kennedy MB (1996) Identification of a phosphorylation site for calcium/calmodulindependent protein kinase II in the NR2B subunit of the N-methyl-D-aspartate receptor. J Biol Chem 271:31670–31678.
Opitz-Araya X, Barria A (2011) Organotypic hippocampal slice cultures. J Vis Exp 48:e2462.
Park M, Penick EC, Edwards JG, Kauer JA, Ehlers MD (2004) Recycling endosomes supply AMPA receptors for LTP. Science 305:1972–1975.
Penn AC, Zhang CL, Georges F, Royer L, Breillat C, Hosy E, Petersen JD, Humeau Y, Choquet D (2017) Hippocampal LTP and contextual learning require surface diffusion of AMPA receptors. Nature 549:384–388.
Philpot BD, Sekhar AK, Shouval HZ, Bear MF (2001) Visual experience and deprivation bidirectionally modify the composition and function of NMDA receptors in visual cortex. Neuron 29:157–169.
Prybylowski K, Chang K, Sans N, Kan L, Vicini S, Wenthold RJ (2005) The synaptic localization of NR2B-containing NMDA receptors is controlled by interactions with PDZ proteins and AP-2. Neuron 47:845–857.
Prybylowski K, Fu Z, Losi G, Hawkins LM, Luo J, Chang K, Wenthold RJ, Vicini S (2002) Relationship between availability of NMDA receptor subunits and their expression at the synapse. J Neurosci 22:8902–8910.
Quinlan EM, Olstein DH, Bear MF (1999a) Bidirectional, experience-dependent regulation of N-methyl-D-aspartate receptor subunit composition in the rat visual cortex during postnatal development. Proc Natl Acad Sci U S A 96:12876–12880.
Quinlan EM, Philpot BD, Huganir RL, Bear MF (1999b) Rapid, experience-dependent expression of synaptic NMDA receptors in visual cortex in vivo. Nat Neurosci 2:352–357.
Roche KW, Standley S, McCallum J, Dune Ly C, Ehlers MD, Wenthold RJ (2001) Molecular determinants of NMDA receptor internalization. Nat Neurosci 4:794–802.
Sanchez JT, Seidl AH, Rubel EW, Barria A (2012) Control of neuronal excitability by NMDA-type glutamate receptors in early developing binaural auditory neurons. J Physiol 590:4801–4818.
Sanchez JT, Wang Y, Rubel EW, Barria A (2010) Development of glutamatergic synaptic transmission in binaural auditory neurons. J Neurophysiol 104:1774–1789.
Sanhueza M, McIntyre CC, Lisman JE (2007) Reversal of synaptic memory by Ca2+/calmodulin-dependent protein kinase II inhibitor. J Neurosci 27: 5190–5199.
Sanz-Clemente A, Matta JA, Isaac JT, Roche KW (2010) Casein kinase 2 regulates the NR2 subunit composition of synaptic NMDA receptors. Neuron 67:984–996.
Schmitt JM, Wayman GA, Nozaki N, Soderling TR (2004) Calcium activation of ERK mediated by calmodulin kinase I. J Biol Chem 279:24064–24072.
Single FN, et al. (2000) Dysfunctions in mice by NMDA receptor point mutations NR1(N598Q) and NR1(N598R). J Neurosci 20:2558–2566.
Stocca G, Vicini S (1998) Increased contribution of NR2A subunit to synaptic NMDA receptors in developing rat cortical neurons. J Physiol 507:13–24.
Storey GP, Opitz-Araya X, Barria A (2011) Molecular determinants controlling NMDA receptor synaptic incorporation. J Neurosci 31: 6311–6316.
Strack S, McNeill RB, Colbran RJ (2000) Mechanism and regulation of calcium/calmodulin-dependent protein kinase II targeting to the NR2B subunit of the N-methyl-D-aspartate receptor. J Biol Chem 275:23798–23806.
Tovar KR, McGinley MJ, Westbrook GL (2013) Triheteromeric NMDA receptors at hippocampal synapses. J Neurosci 33:9150–9160.
Traynelis SF, et al. (2010) Glutamate receptor ion channels: structure, regulation, and function. Pharmacol Rev 62:405–496.
Woods G, Zito K (2008) Preparation of gene gun bullets and biolistic transfection of neurons in slice culture. J Vis Exp 12:e675.
Yashiro K, Philpot BD (2008) Regulation of NMDA receptor subunit expression and its implications for LTD, LTP, and metaplasticity. Neuropharmacology 55:1081–1094.
Zhang S, Edelmann L, Liu J, Crandall JE, Morabito MA (2008) Cdk5 regulates the phosphorylation of tyrosine 1472 NR2B and the surface expression of NMDA receptors. J Neurosci 28:415.
Zhou Y, Takahashi E, Li W, Halt A, Wiltgen B, Ehninger D, Li GD, Hell JW, Kennedy MB, Silva AJ (2007) Interactions between the NR2B receptor and CaMKII modulate synaptic plasticity and spatial learning. J Neurosci 27:13843–13853.